

Oscillon of ultra-light axion-like particle

Masahiro Kawasaki,^{a,b} Wakutaka Nakano^{a,b}
and Eisuke Sonomoto^{a,b}

^aICRR, University of Tokyo,
Kashiwa, 277-8582, Japan

^bKavli IPMU (WPI), UTIAS, University of Tokyo,
Kashiwa, 277-8583, Japan

E-mail: kawasaki@icrr.u-tokyo.ac.jp, m156077@icrr.u-tokyo.ac.jp,
sonomoto@icrr.u-tokyo.ac.jp

Received October 4, 2019

Accepted January 6, 2020

Published January 22, 2020

Abstract. Ultra-Light axion-like particle (ULAP) is one of the attractive candidates for cold dark matter. Because the de Broglie wavelength of ULAP with mass $\sim 10^{-22}$ eV is $\mathcal{O}(\text{kpc})$, the suppression of the small scale structure by the uncertainty principle can solve the core-cusp problem. Frequently, ULAP is assumed to be uniformly distributed in the present universe. In typical ULAP potentials, however, strong self-resonance at the beginning of oscillation invokes the large fluctuations, which may cause the formation of the dense localized object, oscillon. In this paper, we confirm the oscillon formation in a ULAP potential by numerical simulation and analytically derive its lifetime.

Keywords: axions, dark matter simulations, physics of the early universe

ArXiv ePrint: [1909.10805](https://arxiv.org/abs/1909.10805)

Contents

1	Introduction	1
2	Oscillon of ultra-light axion particle	2
2.1	Oscillon solution	2
2.2	Instability growth	4
3	Oscillon formation	4
3.1	Simulation setup	4
3.2	Simulation results	5
4	Oscillon lifetime	6
5	Conclusions	7

1 Introduction

Identifying the dark matter is the issue of greatest concern both in particle physics and cosmology. Amongst various models, cosmological constant and cold dark matter (Λ CDM) model is the most favored by many observations [1, 2].

Λ CDM model significantly succeeds in explaining large-scale structure of the universe though, it still has astronomical problems in small scales. One of the famous problems is the core-cusp problem, in which the tension between the simulated cusp profile [3–5] and observed cored profile of the galactic center [6–8] is reported. This problem is solved, for example, when dark matter is ultra-light ($m \sim 10^{-22}$ eV) and coherently oscillating [9, 10]. This is because the large de Broglie wavelength of the ultra-light particle, approximately the same scale as the galactic center (\sim kpc), smears out the central excessive density. This particle is often called ultra-light axion-like particle (ULAP) because it is ultra-light and coherently oscillating like QCD axion [11–13].

In this case, clumps of ULAP can be formed by the gravity interaction like axion star [14] (we call it “ULA star” with an analogy to QCD axion). ULA star is a kind of soliton that the attractive forces from gravity and repulsive forces from the kinetic pressure are balanced. Some studies show that ULAP forms ULA star by gravity interaction at the galactic center [15–17]. The existence of the star solution is also proved in the contest of axion [18–20] (the axion star formation is also confirmed in ref. [21]).

Before the ULA star formation, however, self-interaction of ULAP can lead to the oscillon [22–24] formation by parametric resonance [25–28] in the radiation dominated universe. Oscillon is a spatially localized solitonic state of a real scalar field, which often survives for a long time because of the conservation of the adiabatic invariance [29, 30]. The existence of such dense objects in the universe affects the current observational constraint [31–37] and proposed experiments [38, 39].

The possibility of long lifetime oscillons in a ULAP potential is pointed out in ref. [40], but their formation and precise lifetime is unclear because analytical estimation of the fluctuation growth and the lifetime is difficult. In this paper, we confirm the oscillon formation by classical lattice simulation in a particular parameter region. We also calculate the oscillon

lifetime by the analytical method derived in ref. [41], which shows that produced ULAP oscillons live long, maybe up to the present day.

In section 2, we show that the condition for the oscillon formation is satisfied in a typical ULAP potential. In section 3, we numerically confirm the oscillon formation by the classical lattice simulation. In section 4, we analytically derive the lifetime of produced oscillon and briefly discuss the cosmological consequence. Finally, in section 5, we conclude our results.

2 Oscillon of ultra-light axion particle

In the context of ULAP, we often use the cosine potential with an analogy to axion. In that case, however, large initial fluctuations are necessary for the oscillon formation because the instability generated by the cosine potential is too weak to enhance the fluctuations. In addition, the resultant oscillon is unstable (the lifetime is $\mathcal{O}(100)m$) [42] and hardly leave interesting cosmological effects [43, 44].

Still many other potentials of ULAP are suggested [45–48], instead of the cosine potential we use the following potential [49–51]

$$V(\phi) = \frac{m^2 F^2}{2p} \left[1 - \left(1 + \frac{\phi^2}{F^2} \right)^{-p} \right], \quad (p > -1) \quad (2.1)$$

where $p > -1$ is necessary to guarantee the existence of the oscillon solution (see 2.1 and eq. (2.9)). In the following subsections, we will show that the two general conditions necessary for the oscillon formation are satisfied;

1. The existence of the oscillon solution,
2. The large fluctuations $\delta\phi/\phi_0 \sim \mathcal{O}(1)$.

Note that these conditions are not sufficient but just necessary. To confirm the oscillon formation, we should perform classical lattice simulation.

2.1 Oscillon solution

First, let us show that the oscillon configuration can be realized in the potential eq. (2.1).

Oscillon is the non-topological pseudo soliton approximately conserving the adiabatic invariant I [29] defined as

$$I \equiv \frac{1}{\omega} \int d^3x \overline{\dot{\phi}^2}, \quad (2.2)$$

where the overline represents the time average over periodic motion of ϕ and ω does its oscillation frequency almost the same as the mass of ϕ .

The oscillon configuration is obtained by minimizing the time-averaged energy \overline{E} for a given I . With the use of the Lagrangian multiplier method,

$$E_\lambda = \overline{E} + \lambda \left(I - \frac{1}{\omega} \int d^3x \overline{\dot{\phi}^2} \right), \quad (2.3)$$

$$= \int d^3x \left[\left(1 - \frac{2\lambda}{\omega} \right) \frac{1}{2} \overline{\dot{\phi}^2} + \frac{1}{2} \overline{(\nabla\phi)^2} + \overline{V(\phi)} \right] + \lambda I. \quad (2.4)$$

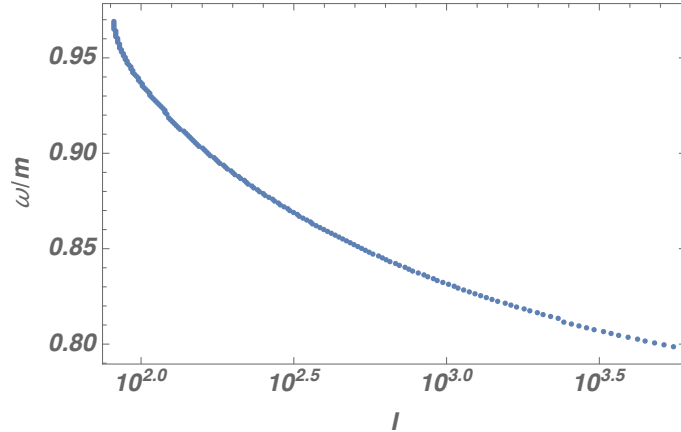


Figure 1. The relation between ω and the adiabatic invariant I . From this figure, ω and I are inversely related, that is, larger ω leads to the oscillon with smaller adiabatic invariant.

Assuming that the periodic motion of ϕ is written as $\phi(x) \simeq \Phi(\mathbf{x}) \cos \omega t$ and defining $V(\Phi) \equiv 2\overline{V(\phi)}$, eq. (2.4) becomes

$$E_\lambda = \frac{1}{2} \int d^3x \left[\omega(\omega - 2\lambda) \frac{1}{2} \Phi^2 + \frac{1}{2} (\nabla \Phi)^2 + V(\Phi) \right] + \lambda I, \quad (2.5)$$

$$= \frac{1}{2} \int d^3x \left[\frac{1}{2} (\nabla \Phi)^2 + V(\Phi) - \frac{1}{2} \omega^2 \Phi^2 \right] + \omega I. \quad (2.6)$$

where we use the relation $\lambda = \omega$ [41] in the last line. Because the lowest energy configuration is realized in the spherically symmetric configuration, we set $\Phi(\mathbf{x}) = \Phi(r)$ and impose the boundary condition as

$$\Phi|_{r \rightarrow \infty} = 0, \quad \left. \frac{d\Phi}{dr} \right|_{r \rightarrow 0} = 0. \quad (2.7)$$

Under this condition, by differentiating E_ω by Φ to get the extremum we obtain

$$\frac{d^2 \Phi}{dr^2} + \frac{2}{r} \frac{d\Phi}{dr} + \frac{d}{d\Phi} \left(\frac{1}{2} \omega^2 \Phi^2 - V(\Phi) \right) = 0. \quad (2.8)$$

This equation is considered as the equations of motion of Φ moving in the potential $\omega^2 \Phi^2 / 2 - V(\Phi)$ with friction. Thus the condition for the solution existence of eq. (2.8) satisfying the boundary condition eq. (2.7) is

$$\min \left[\frac{V(\Phi)}{\Phi^2} \right] < \omega^2 < m^2. \quad (2.9)$$

Because the ULAP potential eq. (2.1) of $p > -1$ satisfies eq. (2.9), the oscillon configuration is realized when the ULAP fluctuations are large enough.

By solving eq. (2.8) in various ω , we derived the relation between ω and the adiabatic invariant I in figure 1. From this figure, we can easily find the inverse relation between ω and the adiabatic invariant I .

2.2 Instability growth

Not only the existence of the oscillon solution but also the large spatial inhomogeneity is necessary for the oscillon formation. In the ULAP case, however, the field value is almost uniform at the beginning of the oscillation because the homogeneous initial value is set by inflation. Therefore, we discuss the growth of the small initial fluctuations by Floquet analysis in this subsection.

For analytical purposes, we expand the potential eq. (2.1) up to a quartic order under $\phi < F$,

$$V(\phi) \simeq \frac{m^2 F^2}{2} \left(\frac{\phi^2}{F^2} - \frac{p+1}{2} \frac{\phi^4}{F^4} \right). \quad (2.10)$$

Assuming that the background is dominated by the harmonic oscillation $\phi_0 \simeq \Phi \cos(mt)$, the equation of motion of the k -mode fluctuations without cosmic expansion leads to the Mathieu equation,

$$\delta\ddot{\phi}_k + [k^2 + V''(\phi_0)] \delta\phi_k = 0, \quad (2.11)$$

$$\Leftrightarrow \delta\ddot{\phi}_k + \left[k^2 + m^2 - \frac{3(p+1)}{2} m^2 \left(\frac{\Phi}{F} \right)^2 (1 + \cos 2mt) \right] \delta\phi_k \simeq 0. \quad (2.12)$$

When $\Phi \lesssim F$, the narrow instability band is induced with the approximate growth rate (Floquet exponent)

$$\frac{\mu_{\max}}{m} \simeq \frac{3(p+1)}{8} \left(\frac{\Phi}{F} \right)^2, \quad \text{at} \quad \frac{k}{m} \simeq \sqrt{\frac{3(p+1)}{2}} \frac{\Phi}{F}, \quad (2.13)$$

which shows that the larger p leads to the stronger instability.¹ In an expanding universe, when $\mu_{\max}/H \gtrsim 1$, the fluctuation growth beats the cosmic expansion and it can lead to large enough fluctuations for the oscillon formation.

3 Oscillon formation

In this section, we verify the oscillon production by the classical lattice simulation after a brief explanation of the simulation setup. The oscillon formation in the potential eq. (2.1) is confirmed in many papers in the inflationary context [52–55]. Here, we test the formation in the radiation dominated universe.

3.1 Simulation setup

In the simulation, the units of the field, time, space, etc. are taken to be F and m^{-1} , that is,

$$\bar{\phi} \equiv \frac{\phi}{F}, \quad \bar{\tau} \equiv m\tau, \quad \bar{x} \equiv mx, \quad \dots \text{ etc.} \quad (3.1)$$

where the overline denotes the dimensionless program variables and τ is the conformal time.

The equation of motion of $\bar{\phi}$ is represented by

$$\bar{\phi}'' + 2\frac{a'}{a}\bar{\phi}' - \bar{\Delta}\bar{\phi} + a^2\frac{\partial\bar{V}}{\partial\bar{\phi}} = 0, \quad \bar{V} = \frac{1}{2p} \left[1 - (1 + \bar{\phi}^2)^{-p} \right]. \quad (3.2)$$

where dash denotes the derivative of $\bar{\tau}$. As the initial condition,

¹See ref. [40] for Floquet exponent of other p .

p	varying
Initial field value $\langle \bar{\phi}_i \rangle$	$2\pi/3$
Box size L	8
Grid size N	256^3
Time	1–50
Time step	0.01

Table 1. Simulation parameters. p is changed in every simulation to test various potentials.

- Hubble parameter: ULAP starts to oscillate in the radiation dominated universe, so we take $H_i = 1/2t = m$.
- Scale factor: the initial scale factor is set to be unity $a_i = 1$. (in the radiation dominated universe $a = \bar{\tau}$).
- Field values: the initial field value and its derivative are set as

$$\bar{\phi}_i = \frac{2}{3}\pi(1 + \zeta), \quad \bar{\phi}'_i = 0. \quad (3.3)$$

where ζ is the uniform random fluctuations of $\mathcal{O}(10^{-5})$.²

The other simulation parameters are shown in table 1.

We utilize our lattice simulation code used in refs. [41, 56], in which the time evolution is calculated by the fourth-order symplectic integration scheme and the spatial derivatives are calculated by the fourth-order central difference scheme. We impose the periodic boundary condition on the boundary.

3.2 Simulation results

The simulation results are shown in figure 2 for $p = 2.5$ (left) and $p = 4$ (right).

In both cases, the high energy local objects are produced. However, we have confirmed by simulations that the oscillon formation does not occur when $p \lesssim 2$. There are two main reasons for this. The first is that smaller p leads to the weaker resonance as shown in eq. (2.13). The twice larger μ after few oscillations makes fluctuations $e^{10} \sim 10^4$ times larger. The second is that the effective mass at the beginning of the oscillation $m_{\text{eff}}^2 = V''(\phi_i)$ becomes smaller in larger p . This causes the later onset of the oscillation, which leads to the increase of the number of oscillations in each Hubble time and instability enhancement.

We also comment on the initial field value. In this simulation, we set $\langle \bar{\phi}_i \rangle = 2\pi/3$ as the benchmark of the $\mathcal{O}(1)$ initial field value. However, if we assume the highly fine-tuned initial condition as $\langle \bar{\phi}_i \rangle = \mathcal{O}(10^{-1})$ or so, fluctuations may not be grown enough because of the opposite reasons to the above two. On the other hand, if we assume the larger initial value, even smaller p may cause the oscillon formation.

Although we focused only on the potential eq. (2.1) in this paper, other ULAP potentials satisfying the condition eq. (2.9) also have the possibility of the oscillon formation.

²The initial field average $\langle \bar{\phi}_i \rangle = 2\pi/3$ is just the benchmark.

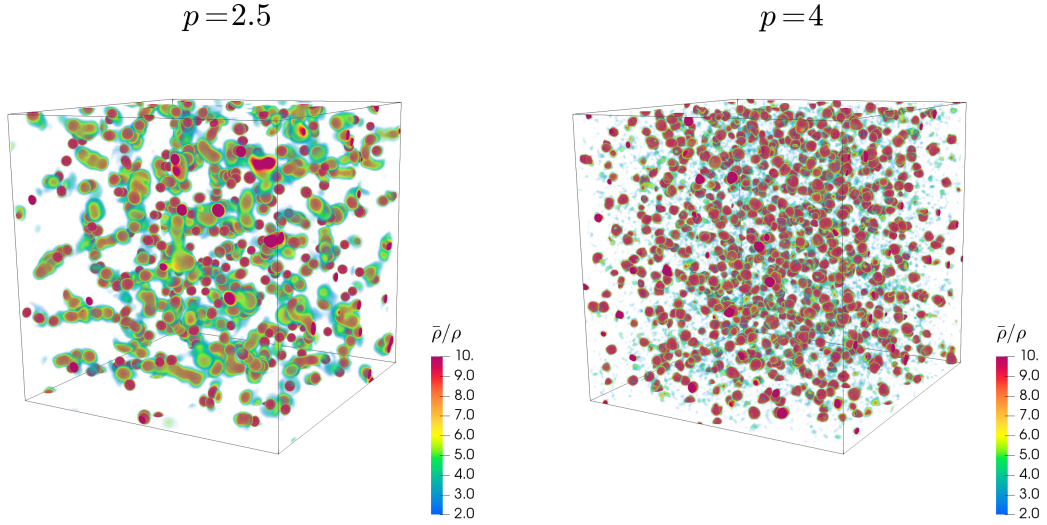


Figure 2. Simulation results. We plot the ratio of the energy density ρ to the averaged one $\bar{\rho}$ in the simulation box at $a = 30$. Left and right figures show the case of $p = 2.5$ and 4 respectively. From these figures, We can find that a lot of oscillons are produced by self-resonance.

4 Oscillon lifetime

In this section, we briefly estimate the oscillon lifetime based on ref. [41] and discuss the effect of the resultant oscillon.

In ref. [41], we derive the method to calculate the classical decay rate of oscillon by solving the equation of motion of fluctuations around the theoretical oscillon profile. Let us decompose a scalar field $\phi(x)$ into the oscillon profile and fluctuations as

$$\phi(x) = 2\psi(r) \cos \omega t + \xi(x). \quad (4.1)$$

where $\psi(r)$ obeys the oscillon profile equation eq. (2.8).³ With the use of the equation of motion of ϕ and eq. (2.8), we drive the equation of motion of ξ as

$$(\square + m^2)\xi(r) = \overline{V'(\psi)} \cos \omega t - V'(\phi). \quad (4.2)$$

Then, approximating the potential V as

$$V'(\phi) \simeq V'(2\psi \cos \omega t), \quad (4.3)$$

and expanding V and \overline{V} about ψ/F to the sixth-order under $\psi \ll F$, we can analytically solve eq. (4.2) by the Green function method. Using the solution of ξ , the energy loss rate of oscillon

$$\frac{dE}{dt} = 4\pi r^2 T^{0r}, \quad (4.4)$$

is calculated where $T_{0r} = \partial_0 \xi \partial_r \xi$ denotes the Poynting vector.

The derived decay rate $\Gamma = |\dot{E}|/E$ is shown in figure 3. As we mentioned in section 2.1, ω relates the oscillon profile and larger ω corresponds to a smaller oscillon (see figure 1). Thus, by emitting the self-radiation oscillons are getting smaller over time, that is, larger ω ,

³We impose the spherical symmetry on the system because we focus only on the lowest energy state.

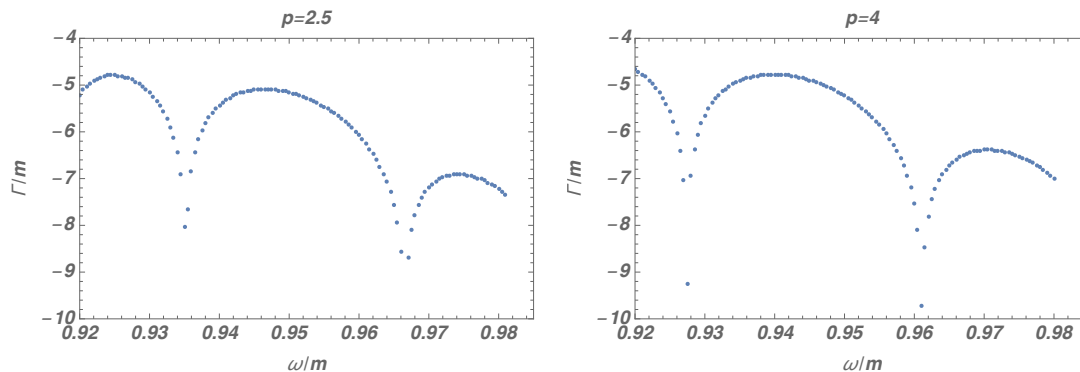


Figure 3. The decay rate of oscillon. The left and right figures show the case of $p = 2.5, 4$ respectively. For $\omega \gtrsim 0.98$ the oscillon does not satisfy the stability condition $\frac{\partial \omega}{\partial I} < 0$ [57]. Larger ω means the smaller oscillon by definition, so the minimum lifetime is $\mathcal{O}(10^7)m$. In addition, if larger oscillons (e.g., $\omega \lesssim 0.96$) are formed, the lifetime may be much longer because the decay rate becomes much smaller there.

which means the decay rate evolves following the curve in figure 3 from left to right. As you can see from figure 3, it is found that the produced oscillon is stable at least for $\mathcal{O}(10^7)m$ when it is small (i.e. $\omega \gtrsim 0.969$ for $p = 2.5$ and $\omega \gtrsim 0.962$ for $p = 4$). Their lifetime is about 10^6 years for the typical ULAP mass $m \sim 10^{-22}$ eV. Such long-lived objects may affect the cosmic evolution, particularly structure formation.

In addition, the lifetime of oscillon may become longer because its lifetime depends on its size. As shown in the figures, the decay rate has a lot of poles where the decay rate is extremely small. At these points, oscillon hardly evolves to the smaller one, which results in a longer lifetime ($\gtrsim 10^{10}$ years).⁴ Therefore, if the large oscillons are formed, ULAP oscillons may still live in the present universe.

5 Conclusions

In this paper, we have examined the oscillon formation in a ULAP potential, eq. (2.1). We have shown that oscillons are really produced when the potential index is $p > 2$ with $\langle \phi_i \rangle / F = 2\pi/3$. Their lifetime is at least $\mathcal{O}(10^7)m$, which equals to 10^6 years with $m \sim 10^{-22}$ eV. Because such long lifetime objects survive until the structure formation, they may affect the dynamical history of the universe.

Moreover, the lifetime could be much longer if large oscillons are formed because the decay rate of the oscillon extremely decreases in the specific profiles. In either case, a deep understanding of the evolution of ULAP oscillons is indispensable to consider effects on cosmology. A detailed study should be discussed in the future work.

Acknowledgments

This work was supported by JSPS KAKENHI Grant Nos. 17H01131 (M.K.) and 17K05434 (M.K.), MEXT KAKENHI Grant Nos. 15H05889 (M.K.), World Premier International Research Center Initiative (WPI Initiative), MEXT, Japan, and JSPS Research Fellowships for Young Scientists Grant No. 19J12936 (E.S.).

⁴Note that the decay rate is probably much smaller than you see from the figures because the plots are discretized for the computational time.

References

- [1] WMAP collaboration, *Seven-year Wilkinson Microwave Anisotropy Probe (WMAP) observations: cosmological interpretation*, *Astrophys. J. Suppl.* **192** (2011) 18 [[arXiv:1001.4538](#)] [[INSPIRE](#)].
- [2] PLANCK collaboration, *Planck 2018 results. VI. Cosmological parameters*, [arXiv:1807.06209](#) [[INSPIRE](#)].
- [3] J.F. Navarro, C.S. Frenk and S.D.M. White, *A universal density profile from hierarchical clustering*, *Astrophys. J.* **490** (1997) 493 [[astro-ph/9611107](#)] [[INSPIRE](#)].
- [4] T. Fukushige and J. Makino, *On the origin of cusps in dark matter halos*, *Astrophys. J.* **477** (1997) L9 [[astro-ph/9610005](#)] [[INSPIRE](#)].
- [5] T. Ishiyama et al., *The cosmogrid simulation: statistical properties of small dark matter halos*, *Astrophys. J.* **767** (2013) 146 [[arXiv:1101.2020](#)] [[INSPIRE](#)].
- [6] A. Borriello and P. Salucci, *The dark matter distribution in disk galaxies*, *Mon. Not. Roy. Astron. Soc.* **323** (2001) 285 [[astro-ph/0001082](#)] [[INSPIRE](#)].
- [7] G. Gilmore et al., *The observed properties of dark matter on small spatial scales*, *Astrophys. J.* **663** (2007) 948 [[astro-ph/0703308](#)] [[INSPIRE](#)].
- [8] S.-H. Oh et al., *High-resolution dark matter density profiles of THINGS dwarf galaxies: correcting for non-circular motions*, *Astron. J.* **136** (2008) 2761 [[arXiv:0810.2119](#)] [[INSPIRE](#)].
- [9] W. Hu, R. Barkana and A. Gruzinov, *Cold and fuzzy dark matter*, *Phys. Rev. Lett.* **85** (2000) 1158 [[astro-ph/0003365](#)] [[INSPIRE](#)].
- [10] L. Hui, J.P. Ostriker, S. Tremaine and E. Witten, *Ultralight scalars as cosmological dark matter*, *Phys. Rev. D* **95** (2017) 043541 [[arXiv:1610.08297](#)] [[INSPIRE](#)].
- [11] S. Weinberg, *A new light boson?*, *Phys. Rev. Lett.* **40** (1978) 223 [[INSPIRE](#)].
- [12] F. Wilczek, *Problem of strong P and T invariance in the presence of instantons*, *Phys. Rev. Lett.* **40** (1978) 279 [[INSPIRE](#)].
- [13] M. Dine, W. Fischler and M. Srednicki, *A simple solution to the strong CP problem with a harmless axion*, *Phys. Lett. B* **104** (1981) 199.
- [14] E.W. Kolb and I.I. Tkachev, *Axion miniclusters and Bose stars*, *Phys. Rev. Lett.* **71** (1993) 3051 [[hep-ph/9303313](#)] [[INSPIRE](#)].
- [15] H.-Y. Schive, T. Chiueh and T. Broadhurst, *Cosmic structure as the quantum interference of a coherent dark wave*, *Nature Phys.* **10** (2014) 496 [[arXiv:1406.6586](#)] [[INSPIRE](#)].
- [16] H.-Y. Schive et al., *Understanding the core-halo relation of quantum wave dark matter from 3d simulations*, *Phys. Rev. Lett.* **113** (2014) 261302 [[arXiv:1407.7762](#)] [[INSPIRE](#)].
- [17] J. Veltmaat, J.C. Niemeyer and B. Schwabe, *Formation and structure of ultralight bosonic dark matter halos*, *Phys. Rev. D* **98** (2018) 043509 [[arXiv:1804.09647](#)] [[INSPIRE](#)].
- [18] E. Braaten, A. Mohapatra and H. Zhang, *Dense axion stars*, *Phys. Rev. Lett.* **117** (2016) 121801 [[arXiv:1512.00108](#)] [[INSPIRE](#)].
- [19] L. Visinelli et al., *Dilute and dense axion stars*, *Phys. Lett. B* **777** (2018) 64 [[arXiv:1710.08910](#)] [[INSPIRE](#)].
- [20] P.-H. Chavanis, *Phase transitions between dilute and dense axion stars*, *Phys. Rev. D* **98** (2018) 023009 [[arXiv:1710.06268](#)] [[INSPIRE](#)].
- [21] D.G. Levkov, A.G. Panin and I.I. Tkachev, *Gravitational Bose-Einstein condensation in the kinetic regime*, *Phys. Rev. Lett.* **121** (2018) 151301 [[arXiv:1804.05857](#)] [[INSPIRE](#)].

- [22] I.L. Bogolyubsky and V.G. Makhankov, *Lifetime of pulsating solitons in some classical models*, *Pisma Zh. Eksp. Teor. Fiz.* **24** (1976) 15 [[INSPIRE](#)].
- [23] M. Gleiser, *Pseudostable bubbles*, *Phys. Rev. D* **49** (1994) 2978 [[hep-ph/9308279](#)] [[INSPIRE](#)].
- [24] E.J. Copeland, M. Gleiser and H.R. Muller, *Oscillons: resonant configurations during bubble collapse*, *Phys. Rev. D* **52** (1995) 1920 [[hep-ph/9503217](#)] [[INSPIRE](#)].
- [25] Y. Shtanov, J.H. Traschen and R.H. Brandenberger, *Universe reheating after inflation*, *Phys. Rev. D* **51** (1995) 5438 [[hep-ph/9407247](#)] [[INSPIRE](#)].
- [26] L. Kofman, A.D. Linde and A.A. Starobinsky, *Nonthermal phase transitions after inflation*, *Phys. Rev. Lett.* **76** (1996) 1011 [[hep-th/9510119](#)] [[INSPIRE](#)].
- [27] L. Kofman, A.D. Linde and A.A. Starobinsky, *Towards the theory of reheating after inflation*, *Phys. Rev. D* **56** (1997) 3258 [[hep-ph/9704452](#)] [[INSPIRE](#)].
- [28] M. Yoshimura, *Catastrophic particle production under periodic perturbation*, *Prog. Theor. Phys.* **94** (1995) 873 [[hep-th/9506176](#)] [[INSPIRE](#)].
- [29] S. Kasuya, M. Kawasaki and F. Takahashi, *I-balls*, *Phys. Lett. B* **559** (2003) 99 [[hep-ph/0209358](#)] [[INSPIRE](#)].
- [30] M. Kawasaki, F. Takahashi and N. Takeda, *Adiabatic invariance of oscillons/I-balls*, *Phys. Rev. D* **92** (2015) 105024 [[arXiv:1508.01028](#)] [[INSPIRE](#)].
- [31] R. Hlozek, D. Grin, D.J.E. Marsh and P.G. Ferreira, *A search for ultralight axions using precision cosmological data*, *Phys. Rev. D* **91** (2015) 103512 [[arXiv:1410.2896](#)] [[INSPIRE](#)].
- [32] M. Viel, G.D. Becker, J.S. Bolton and M.G. Haehnelt, *Warm dark matter as a solution to the small scale crisis: new constraints from high redshift Lyman- α forest data*, *Phys. Rev. D* **88** (2013) 043502 [[arXiv:1306.2314](#)] [[INSPIRE](#)].
- [33] V. Iršič et al., *First constraints on fuzzy dark matter from Lyman- α forest data and hydrodynamical simulations*, *Phys. Rev. Lett.* **119** (2017) 031302 [[arXiv:1703.04683](#)] [[INSPIRE](#)].
- [34] M. Nori et al., *Lyman α forest and non-linear structure characterization in Fuzzy Dark Matter cosmologies*, *Mon. Not. Roy. Astron. Soc.* **482** (2019) 3227 [[arXiv:1809.09619](#)] [[INSPIRE](#)].
- [35] B. Bozek et al., *Galaxy UV-luminosity function and reionization constraints on axion dark matter*, *Mon. Not. Roy. Astron. Soc.* **450** (2015) 209 [[arXiv:1409.3544](#)] [[INSPIRE](#)].
- [36] C. Abel et al., *Search for axionlike dark matter through nuclear spin precession in electric and magnetic fields*, *Phys. Rev. X* **7** (2017) 041034 [[arXiv:1708.06367](#)] [[INSPIRE](#)].
- [37] W.A. Terrano, E.G. Adelberger, C.A. Hagedorn and B.R. Heckel, *Constraints on axionlike dark matter with masses down to 10^{-23} eV/ c^2* , *Phys. Rev. Lett.* **122** (2019) 231301 [[arXiv:1902.04246](#)] [[INSPIRE](#)].
- [38] P.W. Graham et al., *Spin precession experiments for light axionic dark matter*, *Phys. Rev. D* **97** (2018) 055006 [[arXiv:1709.07852](#)] [[INSPIRE](#)].
- [39] K. Nagano, T. Fujita, Y. Michimura and I. Obata, *Axion dark matter search with interferometric gravitational wave detectors*, *Phys. Rev. Lett.* **123** (2019) 111301 [[arXiv:1903.02017](#)] [[INSPIRE](#)].
- [40] J. Ollé, O. Pujolàs and F. Rompineve, *Oscillons and dark matter*, [arXiv:1906.06352](#) [[INSPIRE](#)].
- [41] M. Ibe, M. Kawasaki, W. Nakano and E. Sonomoto, *Decay of I-ball/oscillon in classical field theory*, *JHEP* **04** (2019) 030 [[arXiv:1901.06130](#)] [[INSPIRE](#)].
- [42] B. Piette and W. J. Zakrzewski, *Metastable stationary solutions of the radial d-dimensional sine-Gordon model*, *Nonlinearity* **11** (1998) 1103.

- [43] A. Vaquero, J. Redondo and J. Stadler, *Early seeds of axion miniclusters*, [arXiv:1809.09241](#) [[INSPIRE](#)].
- [44] M. Buschmann, J.W. Foster and B.R. Safdi, *Early-universe simulations of the cosmological axion*, [arXiv:1906.00967](#) [[INSPIRE](#)].
- [45] X. Dong, B. Horn, E. Silverstein and A. Westphal, *Simple exercises to flatten your potential*, *Phys. Rev. D* **84** (2011) 026011 [[arXiv:1011.4521](#)] [[INSPIRE](#)].
- [46] R. Kallosh and A. Linde, *Universality class in conformal inflation*, *JCAP* **07** (2013) 002 [[arXiv:1306.5220](#)] [[INSPIRE](#)].
- [47] R. Kallosh, A. Linde and D. Roest, *Universal attractor for inflation at strong coupling*, *Phys. Rev. Lett.* **112** (2014) 011303 [[arXiv:1310.3950](#)] [[INSPIRE](#)].
- [48] R. Kallosh, A. Linde and D. Roest, *Superconformal inflationary α -attractors*, *JHEP* **11** (2013) 198 [[arXiv:1311.0472](#)] [[INSPIRE](#)].
- [49] E. Silverstein and A. Westphal, *Monodromy in the CMB: gravity waves and string inflation*, *Phys. Rev. D* **78** (2008) 106003 [[arXiv:0803.3085](#)] [[INSPIRE](#)].
- [50] L. McAllister, E. Silverstein and A. Westphal, *Gravity waves and linear inflation from axion monodromy*, *Phys. Rev. D* **82** (2010) 046003 [[arXiv:0808.0706](#)] [[INSPIRE](#)].
- [51] Y. Nomura, T. Watari and M. Yamazaki, *Pure natural inflation*, *Phys. Lett. B* **776** (2018) 227 [[arXiv:1706.08522](#)] [[INSPIRE](#)].
- [52] M.A. Amin et al., *Oscillons after inflation*, *Phys. Rev. Lett.* **108** (2012) 241302 [[arXiv:1106.3335](#)] [[INSPIRE](#)].
- [53] K.D. Lozanov and M.A. Amin, *Self-resonance after inflation: oscillons, transients and radiation domination*, *Phys. Rev. D* **97** (2018) 023533 [[arXiv:1710.06851](#)] [[INSPIRE](#)].
- [54] N. Kitajima, J. Soda and Y. Urakawa, *Gravitational wave forest from string axiverse*, *JCAP* **10** (2018) 008 [[arXiv:1807.07037](#)] [[INSPIRE](#)].
- [55] J.-P. Hong, M. Kawasaki and M. Yamazaki, *Oscillons from pure natural inflation*, *Phys. Rev. D* **98** (2018) 043531 [[arXiv:1711.10496](#)] [[INSPIRE](#)].
- [56] M. Ibe, M. Kawasaki, W. Nakano and E. Sonomoto, *Fragileness of exact I-ball/oscillon*, *Phys. Rev. D* **100** (2020) 125021 [[arXiv:1908.11103](#)] [[INSPIRE](#)].
- [57] K. Mukaida, M. Takimoto and M. Yamada, *On longevity of I-ball/oscillon*, *JHEP* **03** (2017) 122 [[arXiv:1612.07750](#)] [[INSPIRE](#)].